

The Urban Lightning Effect Revealed with Geostationary Lightning Mapper Observations

J.D. Burke¹ and J. Marshall Shepherd¹

¹University of Georgia

December 7, 2022

Abstract

Within the Charlotte, North Carolina, to Atlanta, Georgia, megaregion (Charlanta), the Atlanta metropolitan area has been shown to augment proximal cloud-to-ground (CG) lightning occurrence. Although numerous studies have documented this “urban lightning effect” (ULE) with regard to CG lightning, relatively few have investigated urban effects on distributions of total lightning (TL). Moreover, there has yet to be a study of the ULE using TL observations from the Geostationary Lightning Mapper (GLM). In an effort to fill this gap, we investigated spatial distributions of TL around the cities of Atlanta, GA, Greenville, SC, and Charlotte, NC, using GLM data collected during the warm seasons of 2018–2021. Analyses reveal augmentation of total lightning intensity and frequency over the major cities of Atlanta and Charlotte, with a diminished urban signal over the smaller city of Greenville. This work also demonstrated the potential efficacy of the emerging satellite-based TL climatology in ULE studies.

17 **Abstract**

18 Within the Charlotte, North Carolina, to Atlanta, Georgia, megaregion (Charlanta), the Atlanta
19 metropolitan area has been shown to augment proximal cloud-to-ground (CG) lightning
20 occurrence. Although numerous studies have documented this “urban lightning effect” (ULE) with
21 regard to CG lightning, relatively few have investigated urban effects on distributions of total
22 lightning (TL). Moreover, there has yet to be a study of the ULE using TL observations from the
23 Geostationary Lightning Mapper (GLM). In an effort to fill this gap, we investigated spatial
24 distributions of TL around the cities of Atlanta, GA, Greenville, SC, and Charlotte, NC, using
25 GLM data collected during the warm seasons of 2018–2021. Analyses reveal augmentation of total
26 lightning intensity and frequency over the major cities of Atlanta and Charlotte, with a diminished
27 urban signal over the smaller city of Greenville. This work also demonstrated the potential efficacy
28 of the emerging satellite-based TL climatology in ULE studies.

29 **Plain Language Summary**

30 Studies using ground-based lightning detection networks have revealed an “urban lightning effect”
31 (ULE) around major cities. Recently, the U.S. launched a weather satellite with a unique lightning
32 mapping instrument. This study, possibly for the first time, demonstrated the ability to utilize
33 space-based observation of total lightning to detect the ULE within the Charlotte, North Carolina,
34 to Atlanta, Georgia, urban corridor. The study also paves the way for future ULE analyses as the
35 satellite lightning data record lengthens.

36 **1 Introduction**

37 The “urban lightning effect” (ULE) describes the observed tendency of large urban areas to
38 augment proximal flash occurrence through a variety of hypothesized mechanisms (Shepherd et
39 al., 2015; Stallins and Rose, 2008). Most prominently, major cities display a propensity to modify
40 the convective intensity and associated lightning production of weakly-forced thunderstorms
41 (Ashley et al., 2012; Rose et al., 2008; Stallins and Rose, 2008). As described by Stallins and Rose
42 (2008), anthropogenic influences on flash production can be broadly grouped into two inter-
43 connected categories: (i) enhancement of local surface convergence and convective instability
44 arising from the characteristics of the urban boundary layer heat island (BLHI) and surface
45 morphology and (ii) modification of the microphysical conditions driving cloud electrification by

46 anthropogenic aerosols. More generally, these can be summarized as thermodynamic,
47 morphological, and microphysical “urban effects.”

48 The Charlanta megaregion consists of a rapidly developing Urban Climate Archipelago (UCA)
49 roughly following Interstate-85 between Atlanta, GA, Greenville, SC, and Charlotte, NC.
50 Shepherd et al. (2014) defined a UCA as a chain or aggregate of urban areas that modify aspects
51 of the climate system. As the focus of numerous studies, the city of Atlanta exhibits strong urban
52 augmentation of lightning intensity and frequency (Rose et al., 2008; Stallins and Bentley, 2006;
53 Stallins et al. 2006; Stallins and Rose, 2008). Stallins et al. (2006) found that average annual CG
54 flash densities in Atlanta between 1992–2003 were 50%–75% higher than in surrounding rural
55 areas. Rose et al. (2008) observed a clear relationship between anomalies of precipitation,
56 lightning, and the prevailing wind direction. In an integrated study of radar reflectivity and
57 lightning data focused on Atlanta, Ashley et al. (2012) found statistically significant increases in
58 aggregate (1997–2006) warm season CG flash counts and flash days between defined urban-rural
59 boundaries of 34%–42% and 14%–20%, respectively. A key finding of their study was the linkage
60 between patterns of lightning, precipitation, and the geometry of the urban footprint. Increasing
61 contiguity of impervious surfaces and rapid expansion of urban sprawl are predicted to
62 dramatically alter the spatial footprints of individual cities and the structure of the entire Charlanta
63 UCA in the coming years (Stone et al., 2013; Terando et al., 2014), emphasizing the need for
64 continued investigation and monitoring of the ULE.

65 Though global networks detecting total lightning flashes have been widely operated for many
66 years, regional and continental CG detection networks have been the preferred sources of flash
67 data due to a number of undesirable characteristics associated with lightning detection at a global
68 scale, namely, low detection efficiencies and spatio-temporal variations in accuracy (Hayward et
69 al., 2020; Lay et al., 2005). The now defunct spaceborne Lightning Imaging Sensor (LIS) and its
70 antecedent prototype aboard *MicroLab-1*, known as the Optical Transient Detector (OTD),
71 suffered from similar data accuracy and consistency issues due to the low earth orbit (LEO) of the
72 Tropical Rainfall Measuring Mission (TRMM) satellite, which resulted in discontinuous spatio-
73 temporal coverage and middling detection efficiencies, though still offering substantial
74 improvement over ground-based global networks (Boccippio et al., 2000, 2002; Hayward et al.,
75 2020). In an effort to remedy the known pitfalls of lightning detection via satellites in LEO, NASA

76 and NOAA jointly launched the GLM aboard the Geostationary Operational Environmental
77 Satellite (GOES) R-series in 2016, marking the advent of spatially and temporally continuous
78 lightning detection from space (Goodman et al., 2013; Medici et al., 2017). This novel availability
79 of high-resolution TL data from the GLM presents contemporary researchers of the ULE with a
80 convenient source for reliable TL observations. Nevertheless, there has yet to be an urban lightning
81 study that utilizes data from the GLM in its analysis.

82 As possibly the first study to utilize observations from the GLM to investigate the ULE, the
83 overarching purpose of this study was to provide insight into the utility of GLM data for future
84 analyses of the ULE. Consequently, we used warm season (June, July, August; JJA) flash data
85 from the first four years of GLM observation (2018–2021) to develop and analyze a set of TL
86 climatologies for the Charlanta UCA. A stated objective of the GLM is to provide spatio-
87 temporally continuous lightning observations for use in long-term climatological analyses
88 (Rudlosky et al. 2019; Rudlosky et al. 2020). As it is well established that TL serves as a robust
89 proxy for convective intensity due to the overwhelming predominance of IC flashes relative to CG
90 strikes (MacGorman et al., 2011), we hypothesize that the ULE will be resolvable in TL
91 observations from the GLM.

92 **2 Data**

93 **2.1 GLM observations**

94 The GLM 1372 by 1300 pixel charge-coupled device (CCD) detects near-infrared (NIR) emissions
95 within a narrow 1 nm band centered at 777.4 nm, providing an at-nadir spatial resolution of
96 approximately 8 km (Goodman et al., 2013). Downstream processing by the Lightning Cluster
97 Filter Algorithm (LCFA) clusters the detected lightning “events” into higher order data classes of
98 “groups” and “flashes” (Goodman et al., 2012; Thiel et al., 2020), each containing spatial
99 information in the form of latitude-longitude coordinates. The purpose of a GLM group is to serve
100 as a proxy for the individual return strokes (current discharges) that make up a ground (cloud)
101 flash, while a GLM flash is intended to correspond to a conventional lightning flash (Goodman et
102 al., 2012). Final GLM products have a daytime (nighttime) flash detection efficiency (DE) greater
103 than 70% (90%) and location accuracy of approximately 4 km (Koshak et al., 2018; Rudlosky et
104 al., 2019).

105 Recently, Oda et al. (2022) performed an initial climatological analysis of total flash rate density
106 (FRD) in Brazil using GLM data. In collaboration with the Center for Weather Forecasting and
107 Climate Studies (CPTEC) within Brazil's National Institute for Space Research (INPE),
108 processing by Oda et al. (2022) accumulated more than 6 million provisionally mature 20-second
109 Level 2 (L2) GLM packets into 5-minute bins and spatially aggregated the included events, groups,
110 and flashes on a $0.08^\circ \times 0.08^\circ$ latitude-longitude grid. Quality control measures were taken by
111 filtering GLM observations to those only with a Data Quality Flag of "good," as recommended by
112 Rudlosky et al. (2019). Each gridded file contains the centroid density of the variables produced
113 by the LCFA, representing the total number of flash, group, and event centroids detected within
114 each grid cell over the 5-minute time interval. These products are made publicly available through
115 a managed archive (CPTEC/INPE, 2022).

116 Facilitating the objectives of our study, warm season (JJA) GLM observations were acquired from
117 CPTEC's public archive in their native netCDF format for a 4-year period (2018–2021). The
118 Climate Data Operators (CDO; Schulzweida, 2022) suite of command line tools was utilized to
119 aggregate the 5-minute files, filter to the desired geographic region, and to derive a set of metrics
120 aimed at quantifying TL intensity and frequency over the 4-year period of record: 1) the total FRD
121 (i.e., total flashes $\text{km}^{-2} \text{year}^{-1}$), 2) the total number of active flash days (i.e., days where total flash
122 count ≥ 1), and 3) the average flashes per flash day (i.e., total flashes / flash days).

123 **2.2 Physiographic data**

124 Land cover data was obtained from the United States Geological Survey (USGS) National Land
125 Cover Database (NLCD 2011), which provides access to spatially explicit land cover and per-pixel
126 impervious surface products derived from 30 meter Landsat imagery (Dewitz, 2021; Yang et al.,
127 2018). Additionally, 7.5-arc-second Global Multi-resolution Terrain Elevation Data
128 (GMTED2010) was obtained from the USGS Earth Resources Observation and Science (EROS)
129 Center archive (Danielson and Gesch, 2011; EROS, 2017).

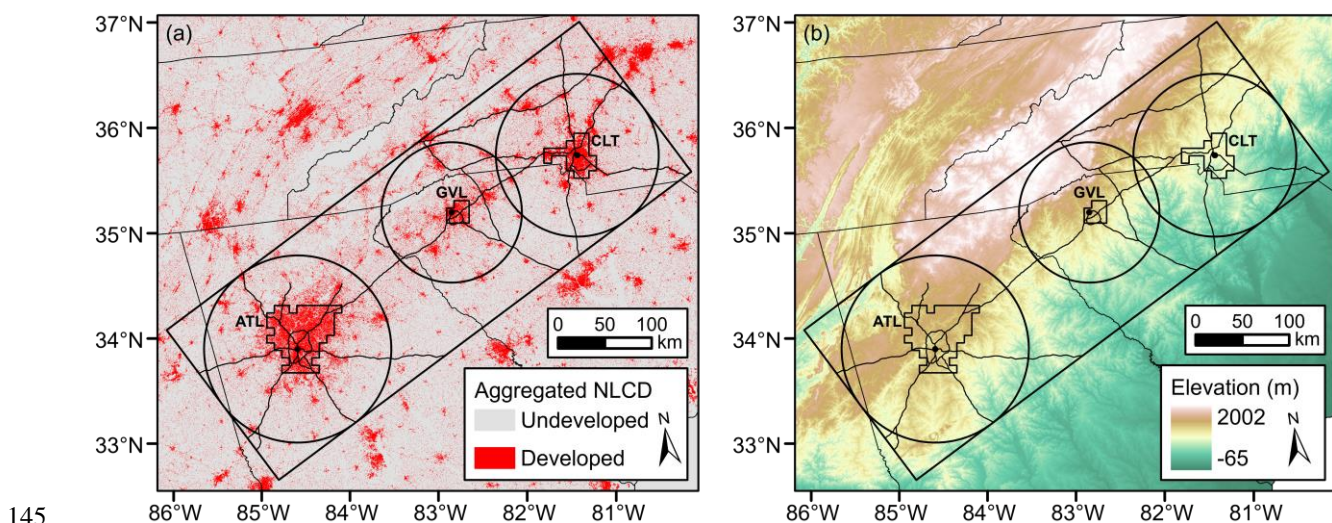
130 **3 Methods**

131 Maps of the derived GLM TL flash metrics were created in ArcGIS Pro 2.9 by converting the
132 gridded latitude-longitude point dataset to raster format and projecting to the Albers Equal-Area
133 Conic (AEAC) projection (Snyder, 1987), resulting in a spatial resolution of approximately 8 km

134 (ESRI, 2021). The following sections describe the steps taken to construct and analyze four-year
 135 warm season TL flash climatologies across the Charlanta megaregion.

136 3.1 Defining the Charlanta megaregion and constituent domains

137 Three city-scale domains centered on Atlanta, Greenville, and Charlotte were constructed using
 138 geometric buffers with radii of 100 km, 75 km, and 87.5 km, respectively. These buffers were
 139 based around each city's administratively defined center to define the outer boundaries of their
 140 domains. A rectangular polygon feature representing the entire Charlanta megaregion was defined
 141 using ArcGIS Pro's *Minimum Bounding Geometry* tool with the three geometric buffers of
 142 Charlanta's major cities as the input features (displayed in Figure 1 below). These boundary
 143 features were used to clip the GLM dataset to the Charlanta megaregion and its constituent city-
 144 scale domains before mapping each TL metric for visual analysis.



146 **Figure 1.** (a): Aggregated 2011 NLCD layer overlaid with the geometric buffers and NLCD-
 147 derived urban delineations constructed to define the domains of Atlanta (ATL), Charlotte (CLT),
 148 and Greenville (GVL). (b) The topography of the Charlanta megaregion (average elevation (m)
 149 within each pixel).

150 3.2 Statistical analysis

151 Providing a more objective assessment of the ULE's presence in GLM TL observations, two
 152 statistical analyses were conducted using the R statistical programming language (R Core Team,
 153 2022). To construct the sampling schema for these analyses, a binary classification method was

154 implemented in ArcGIS Pro using 2011 NLCD land cover areal coverage data to delineate a
155 contiguous urban core sample for each city included in the study. The four developed land cover
156 classes (Developed, Open Space (21); Developed, Low Intensity (22); Developed, Medium
157 Intensity (23); Developed, High Intensity (24)) included in the NLCD raster dataset were spatially
158 aggregated and summarized within the bounds of the vectorized GLM grid cells to form a broad
159 urban/rural percentage. For each GLM grid cell polygon, if the areal coverage of the developed
160 classes was greater than or equal to 50% of the total cell area, the cell was classified as urban,
161 while cells with less than 50% coverage were classified as “rural.” Cells that were classified as
162 urban but disconnected from the urban core were removed, resulting in a conterminous delineation
163 of the urban footprint nested within the outer domain boundary of each city. These delineations
164 served as the urban vs. rural sampling schema for subsequent statistical analyses.

165 Similar to the methodology of Ashley et al. (2012), the averages of the urban and rural TL metrics
166 were compared for each city to assess the magnitude of urban enhancement. Additionally,
167 inferential statistical analyses in the form of independent two-sample t tests were conducted for
168 each city’s urban and rural samples (Student, 1908). An alpha level of 0.05 was used for these
169 tests. Formally, the hypothesis tested was:

170 $H_0 =$ There is no significant difference between the urban and rural samples.

171 $H_1 =$ There is a significant difference between the urban and rural samples.

172 **4 Results**

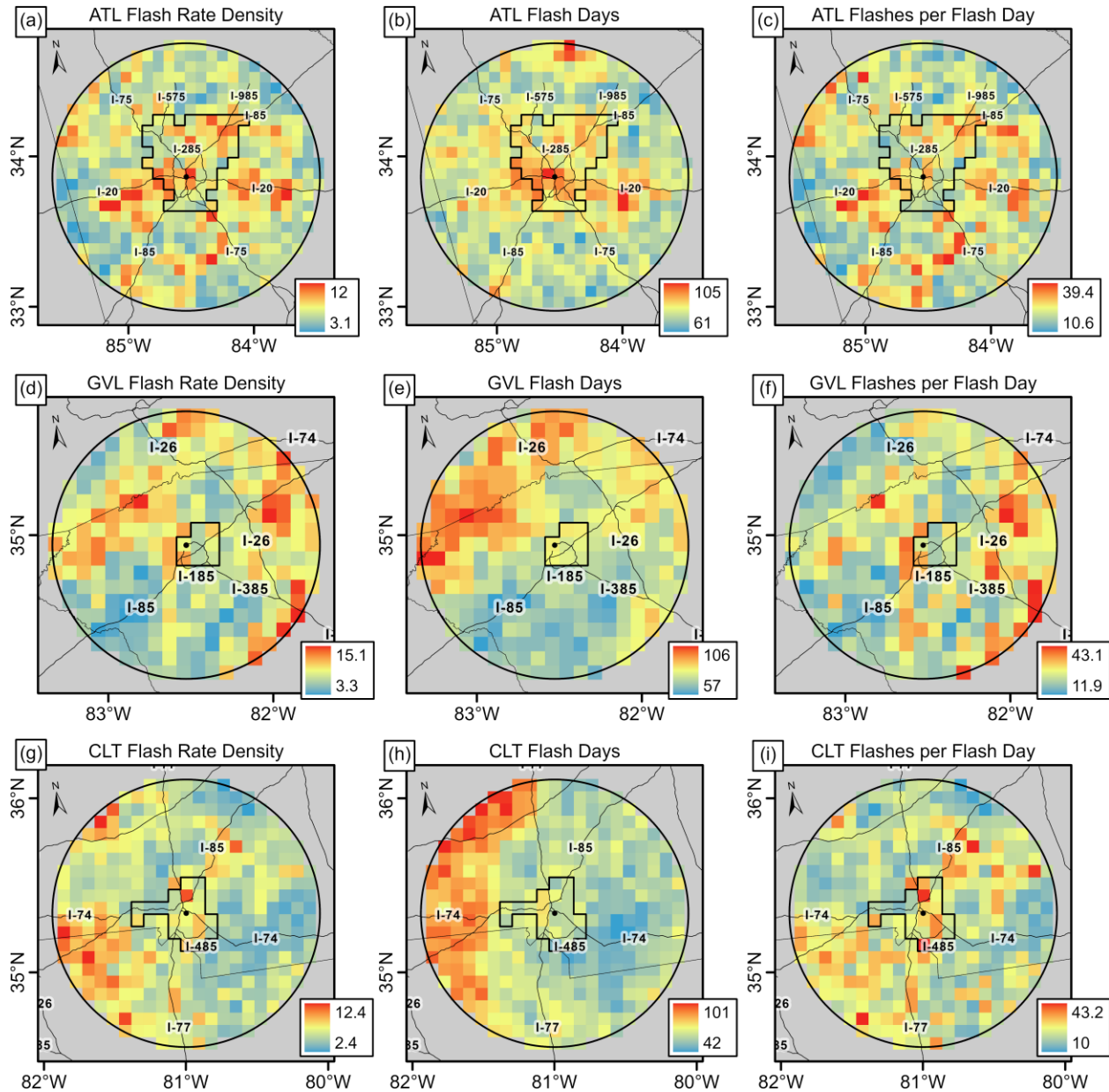
173 Figure 2 displays city-focused maps of the TL metrics derived from GLM observations during the
174 summers of 2018–2021. Figure 3 displays the warm season TL maps created for the Charlanta
175 megaregion and the results of the statistical analyses conducted for each city.

176 The maps of the Atlanta domain (shown in Figures 2a-c and 3a-c) highlight many of the
177 conspicuous patterns observed in past work. Similar to the CG flash distributions examined by
178 Rose et al. (2008) and Ashley et al. (2012), a broad area of TL enhancement is spatially correlated
179 with Atlanta’s sprawling urban footprint and main interstate arteries. Pronounced hotspots in total
180 flash rate density and flash days are visible inside the NLCD-based urban core delineation, though
181 the latter are more strongly clustered within 40 km of the city-center. Average flashes per flash
182 day are also elevated within the urban core delineation, though the most prominent hotspots are

183 located in an arc beginning to the west and ending to the northeast of the city at distances between
184 40–80 km from the city-center.

185 A few distinct features present in all three TL metrics are the hotspots at the intersection of I-85
186 and I-985 near the northeastern extent of the urban delineation and along I-20 between 40-80 km
187 from the city-center. The former was described as the “Gwinnett hotspot” (referring to Gwinnett
188 County) by Stallins and Bentley (2006) in their analysis of warm season CG flash distributions.
189 Diem and Mote (2005) and Diem (2008) also documented nearly coincident enhancement of
190 rainfall in Norcross, GA, within Gwinnett County. Another notable feature is the southwest-to-
191 northeast oriented band of elevated flash rate densities and average flashes per flash day extending
192 approximately 70 km from the city-center, within the corridor of I-85 and I-20. This corridor
193 contains the Chattahoochee River Valley (depicted in Figure 1b), which has been hypothesized to
194 enhance proximal convective activity (McLeod et al., 2017). There is also a hotspot in flash days
195 near the northernmost extent of the domain, likely associated with the rising terrain of the Blue
196 Ridge mountains.

197



198

199 **Figure 2.** Maps of the total flash rate density (flashes $\text{km}^{-2} \text{year}^{-1}$), total flash days, and average
 200 flashes per flash day derived from GLM observations (JJA, 2018–2021) for the cities of Atlanta
 201 (a-c), Greenville (d-f), and Charlotte (g-i).

202 Within the Atlanta domain, assessment of each TL metric's average between the urban and rural
 203 regions (displayed in Figure 3e) revealed increases of 14.3%, 8.3%, and 5.5% for total flash rate
 204 density, flash days, and average flashes per flash day, respectively. The independent samples *t* tests
 205 (results displayed in Figure 3f) found statistically significant ($\alpha = 0.05$) increases in the averages
 206 of total flash rate density and flash days within Atlanta's urban core, but not for average flashes

207 per flash day ($t = 1.88$, $p = .060$). In conjunction with the visual assessment, these results suggest
208 that during the warm season, the urban effects associated with Atlanta's core area of development
209 are strong enough to stimulate both storm-scale flash production and the initiation of
210 thunderstorms that would not have otherwise occurred.

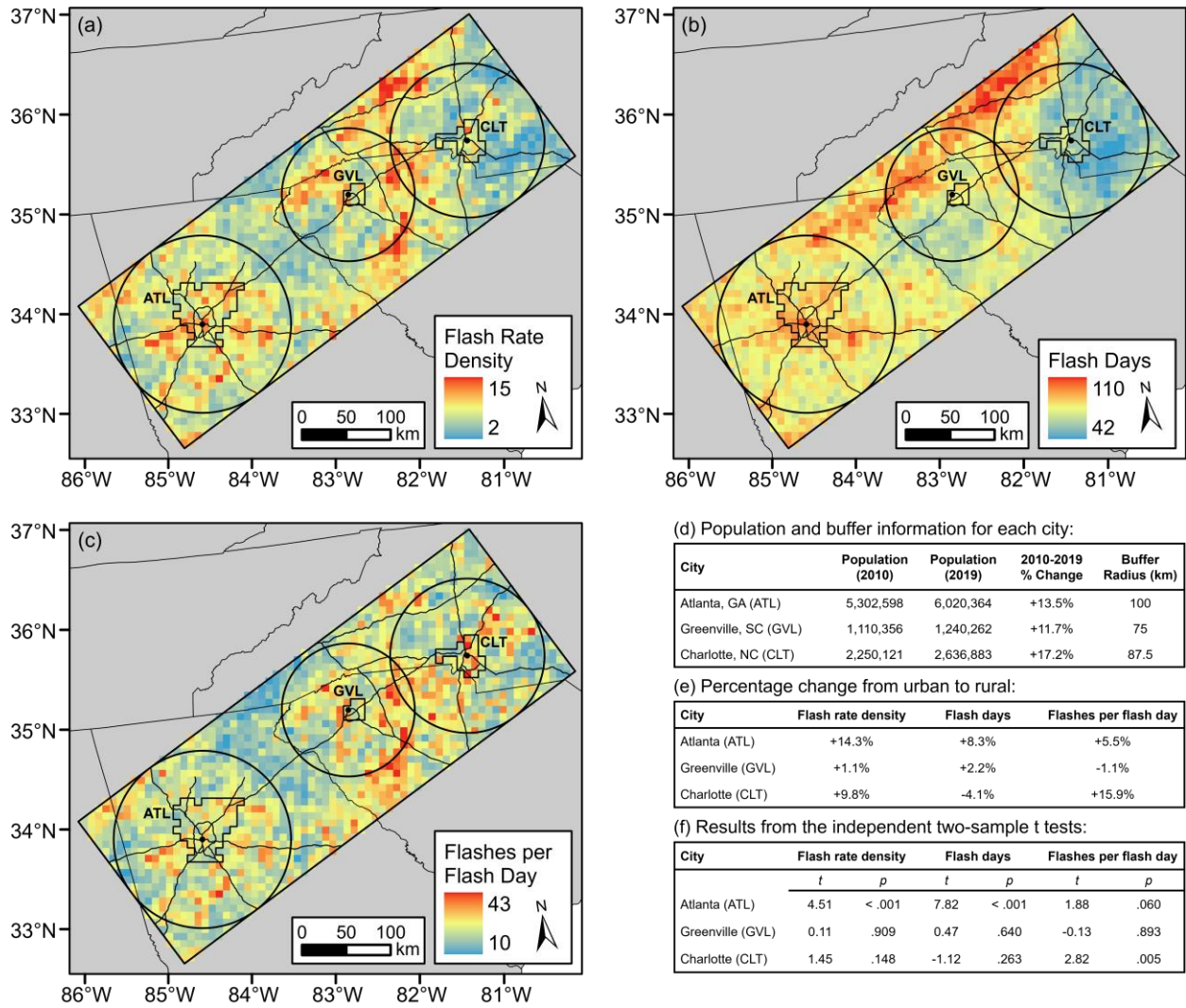
211 In Figures 2d-f and 3a-c, the more moderately sized city of Greenville exhibits a less conspicuous
212 urban influence than that observed in Atlanta. The most prominent areas of elevated total flash rate
213 density and flash days are distributed broadly across the northern half of the domain. These
214 distinctly non-urban features are driven by the local topography as this area of the Greenville
215 domain contains portions of the Blue Ridge Escarpment. Most notable, though, are the hotspots in
216 total flash rate density and average flashes per flash day to the immediate west of Greenville's
217 city-center and along I-85 near the northeastern extent of the domain. Although the latter are well
218 outside the demarcated urban core of Greenville, this section of the I-85 corridor is often downwind
219 of considerable urban sprawl between the twin-cities of Greenville and Spartanburg.

220 Statistical assessment of the Greenville domain found minute differences between the delineated
221 urban and rural regions (shown in Figure 3e), with 1.1% and 2.2% higher average total flash rate
222 density and flash days, respectively, and 1.1% lower average flashes per flash day within the urban
223 core. The t tests found none of these differences to be statistically significant (displayed in Figure
224 3f). The smaller size and spatial density of the Greenville metro area underlie an expectation that
225 its influences will be weaker relative to the dominant geophysical controls on TL production,
226 though Greenville's urban effects are likely to still be a supplementary factor. Nevertheless, it is
227 apparent that our "one-size-fits-all" method of constructing the analysis domains around individual
228 city-centers fails to capture the true urban footprint of the twin-cities arrangement, resulting in
229 contamination of the "rural" sample. This situation also highlights the inadequacy of the GLM's
230 nominal spatial resolution (8 km at-nadir) for analyses of the ULE around small-to-moderately
231 sized cities such as Greenville and Spartanburg, as it lacks the granularity required for finer-scale
232 analysis. Furthermore, the coarse resolution of the utilized GLM dataset results in a limited number
233 of cells being included in the NLCD-based urban delineation.

234 The Charlotte domain (shown in Figures 2g-i and 3a-c) contains hotspots in total flash rate density
235 and average flashes per flash day within the NLCD-based delineation of the urban core and along
236 the west-southwestern periphery of the domain. The latter is an extension of those noted near the

237 northeastern extent of the Greenville domain. Distinct hotspots in total flash rate density and
238 average flashes per flash day are also visible to the northeast of the urban delineation, roughly
239 following the I-85 corridor. While it is quite possible that these anomalies are associated with the
240 typical downwind augmentation process, the heterogeneity of the underlying surface
241 characteristics must be considered as another contributor. Likewise, TL flash days are heavily
242 influenced by the terrain features of the Blue Ridge Mountains across the northwestern extent of
243 the domain. Increases of 9.8% and 15.9% were calculated for the averages of total flash rate density
244 and flashes per flash day, respectively, within the urban core, while the average number of flash
245 days was 4.1% lower (displayed in Figure 3e). Hypothesis testing only found a statistically
246 significant increase in TL flashes per flash day ($t = 2.82, p = .005$), while no significant difference
247 was found for flash rate density and flash days (results displayed in Figure 3f).

248 These results indicate that Charlotte's ULE is manifested most prominently at the storm-scale,
249 with the average TL flash day near the urban core tending to be more electrically active than in the
250 surrounding areas. Similar to the Greenville domain, the urban forcing provided by Charlotte is
251 largely supplementary to natural geophysical factors (e.g., orographic preferences) which act as
252 the dominant controls on the distributions of TL intensity and frequency. While Atlanta's spatially
253 dense and vast urban sprawl displays an ability to initiate thunderstorms that would not have
254 otherwise occurred, Charlotte's smaller urban core likely precludes it from serving as a dominant
255 forcing in thunderstorm initiation and resultant lightning production. As mentioned by McLeod et
256 al. (2017) and Miller et al. (2015), the complex interaction between terrain-related boundary layer
257 processes (e.g., downslope circulations due to differential heating, orographic forcing for ascent)
258 and urban-induced mesocirculations, among other factors, warrant further investigation with
259 improved methods and resources.



260

261 **Figure 3.** Maps of the (a) total flash rate density (flashes km⁻² year⁻¹), (b) flash days, and (c)
 262 average flashes per flash day derived from GLM observations during the warm seasons of 2018–
 263 2021. (d) Population characteristics and buffer size information for each city. (e) Percentage
 264 change in the average of each TL flash metric between the NLCD-derived urban delineation and
 265 surrounding rural region. (f) Results from the independent two-sample *t* tests ($\alpha = 0.05$) for each
 266 domain.

267 **5 Conclusions**

268 This is possibly the first study of the ULE to utilize data collected by the GLM, and therefore, the
 269 first to utilize spatio-temporally continuous TL observations from a satellite platform in
 270 geostationary orbit. Consequently, our primary objective was to determine the utility of GLM data

271 for urban lightning research by analyzing spatial distributions of TL during the warm seasons of
272 2018–2021 around the constituent cities of the Charlanta UCA: Atlanta, GA, Charlotte, NC, and
273 Greenville, SC. Visual and statistical analyses of the aggregated GLM dataset found that several
274 of the spatial patterns noted in previous research were resolvable. Most prominently, significant
275 augmentation of total lightning intensity and frequency was apparent over the major cities of
276 Atlanta and Charlotte, with a diminished urban signal over the smaller city of Greenville. These
277 observations echo the findings of Ashley et al. (2012) and a number of earlier studies (Huff and
278 Changnon, 1973; Oke, 1982; Bentley et al., 2012) that urban morphological characteristics,
279 namely, extent, density, and orientation, are key factors in determining the degree to which
280 lightning occurrence is modified. The products of this study underscore the promise of utilizing
281 TL observations from the GLM in future urban lightning research, while also highlighting certain
282 limitations, the need for improvements to the implemented methodology, and the development of
283 more sophisticated approaches to investigating the ULE.

284 **5.1 Brief discussion of methodological improvements**

285 Though GLM data gridded at its nominal spatial resolution is shown to be less than ideal for robust
286 analyses of the ULE around small-to-moderately sized cities, our work supports its use at the scales
287 of major cities and urban megaregions. This outcome was not entirely unexpected based on the
288 work of Stallins and Rose (2008), which detailed optimal resolutions for such analyses. Though
289 there is precedent for the use of coarser resolution data (e.g., Pinto et al. (2004) used 9 km x 9 km
290 grid cells), it remains insufficient for analyses focused on smaller-scale cities in which the
291 attendant urban effects are predominantly supplementary factors relative to geophysical drivers of
292 total lightning production. In this regard, there are two apparent strategies that could be
293 implemented to improve the effectiveness of future analyses: 1) utilization of the “glmtools” open-
294 source software package, which allows for re-sampling of GLM data to the 2 km x 2 km fixed grid
295 of the Advanced Baseline Imager (Bruning, 2019; Bruning et al., 2019), and 2) the use of more
296 innovative methodologies such as that of Forney et al. (2022), which employed a random forest
297 approach to control for relevant geophysical factors (e.g., elevation, distance from coastline).
298 Despite the acknowledged deficiencies, our analysis documented clear patterns of the ULE
299 observed in past studies, providing the initial support for continued and improved use of GLM data
300 in urban lightning research.

301 **Acknowledgements:**

302 This research was funded by the NASA Interdisciplinary Research in Earth Science (IDS)
303 program (80NSSC20K1268).

304

305 **Data Availability Statement:**

306 GLM data from the CPTEC/INPE archive was used in the creation of this manuscript
307 (CPTEC/INPE, 2022). A complete description of the available GLM data is provided by Oda et
308 al. (2022). The CDO suite of command line tools was utilized to process the acquired GLM data
309 (Schulzweida, 2022). The locally processed GLM data analyzed in this work can be found at
310 <https://doi.org/10.5281/zenodo.7350724>. Land cover data was obtained from the USGS NLCD
311 (Dewitz, 2021; Yang et al., 2018). Global Multi-resolution Terrain Elevation Data was obtained
312 from the EROS archive (Danielson and Gesch, 2011; EROS, 2017). Figures and constituent
313 maps were created with ArcGIS Pro version 2.9 (ESRI, 2021).

314

315 **References:**

- 316 Ashley, W. S., Bentley, M. L., & Stallins, J. A. (2012). Urban-induced thunderstorm modification
317 in the Southeast United States. *Climatic Change*, 113(2), 481–498.
318 <https://doi.org/10.1007/s10584-011-0324-1>
- 319 Bentley, M. L., Ashley, W. S., & Stallins, J. A. (2011). Radar identification of urban-enhanced
320 thunderstorm activity for Atlanta, Georgia, USA. *2011 Joint Urban Remote Sensing Event*,
321 413–416. <https://doi.org/10.1109/JURSE.2011.5764807>
- 322 Bentley, M., Stallins, J., & Ashley, W. (2012). Synoptic environments favourable for urban
323 convection in Atlanta, Georgia. *International Journal of Climatology*, 32.
324 <https://doi.org/10.1002/joc.2344>
- 325 Blakeslee, R. J., & Goodman, S. J. (1992). *Lightning Imaging Sensor (US) for the Earth Observing*
326 *System*. 44.
- 327 Boccippio, D. J., Koshak, W., Blakeslee, R., Driscoll, K., Mach, D., Buechler, D., Boeck, W.,
328 Christian, H. J., & Goodman, S. J. (2000). The Optical Transient Detector (OTD): Instrument
329 Characteristics and Cross-Sensor Validation. *Journal of Atmospheric and Oceanic*

- 330 *Technology*, 17(4), 441–458. <https://doi.org/10.1175/1520->
331 0426(2000)017<0441:TOTDOI>2.0.CO;2
- 332 Boccippio, D. J., Koshak, W. J., & Blakeslee, R. J. (2002). Performance Assessment of the Optical
333 Transient Detector and Lightning Imaging Sensor. Part I: Predicted Diurnal Variability.
334 *Journal of Atmospheric and Oceanic Technology*, 19(9), 1318–1332.
335 [https://doi.org/10.1175/1520-0426\(2002\)019<1318:PAOTOT>2.0.CO;2](https://doi.org/10.1175/1520-0426(2002)019<1318:PAOTOT>2.0.CO;2)
- 336 Bruning, E. (2019). *deeplycloudy/glmtools: Glmtools release to accompany publication*. Zenodo.
337 <https://doi.org/10.5281/zenodo.2648658>
- 338 Bruning, E. C., Tillier, C. E., Edgington, S. F., Rudlosky, S. D., Zajic, J., Gravelle, C., Foster, M.,
339 Calhoun, K. M., Campbell, P. A., Stano, G. T., Schultz, C. J., & Meyer, T. C. (2019).
340 Meteorological Imagery for the Geostationary Lightning Mapper. *Journal of Geophysical*
341 *Research: Atmospheres*, 124(24), 14285–14309. <https://doi.org/10.1029/2019JD030874>
- 342 Changnon, S. A., Huff, F. A., & Semonin, R. G. (1971). METROMEX: An investigation of
343 inadvertent weather modification. *Bulletin of the American Meteorological Society*, 52(10),
344 958–968. [https://doi.org/10.1175/1520-0477\(1971\)052<0958:MAIOIW>2.0.CO;2](https://doi.org/10.1175/1520-0477(1971)052<0958:MAIOIW>2.0.CO;2)
- 345 CPTEC/INPE. (2022). *Accumulated GOES-16 GLM Data* [Data set]. Center for Weather
346 Forecasting and Climate Studies (CPTEC)/National Institute for Space Research (INPE).
347 http://ftp.cptec.inpe.br/goes/goes16/goes16_web/glm_acumulado_nc/
- 348 Danielson, J. J., & Gesch, D. B. (2011). Global multi-resolution terrain elevation data 2010
349 (GMTED2010). In *Global multi-resolution terrain elevation data 2010 (GMTED2010)*
350 (USGS Numbered Series No. 2011–1073; Open-File Report, Vols. 2011–1073). U.S.
351 Geological Survey. <https://doi.org/10.3133/ofr20111073>
- 352 Dewitz, J. (2021). *National Land Cover Database (NLCD) 2019 Products* [Data set]. U.S.
353 Geological Survey. <https://doi.org/10.5066/P9KZCM54>
- 354 Diem, J. E. (2008). Detecting summer rainfall enhancement within metropolitan Atlanta, Georgia
355 USA. *International Journal of Climatology*, 28(1), 129–133.
356 <https://doi.org/10.1002/joc.1560>
- 357 Diem, J. E., & Mote, T. L. (2005). Interepochal Changes in Summer Precipitation in the
358 Southeastern United States: Evidence of Possible Urban Effects near Atlanta, Georgia.
359 *Journal of Applied Meteorology and Climatology*, 44(5), 717–730.
360 <https://doi.org/10.1175/JAM2221.1>

- 361 EROS. (2017). *Global Multi-resolution Terrain Elevation Data 2010 (GMTED2010)* [Data set].
362 U.S. Geological Survey. <https://doi.org/10.5066/F7J38R2N>
- 363 ESRI. (2021). *ArcGIS Pro* (2.9). ESRI. [https://pro.arcgis.com/en/pro-app/latest/tool-](https://pro.arcgis.com/en/pro-app/latest/tool-reference/main/arcgis-pro-tool-reference.htm)
364 [reference/main/arcgis-pro-tool-reference.htm](https://pro.arcgis.com/en/pro-app/latest/tool-reference/main/arcgis-pro-tool-reference.htm)
- 365 Forney, R. K., Debbage, N., Miller, P., & Uzquiano, J. (2022). Urban effects on weakly forced
366 thunderstorms observed in the Southeast United States. *Urban Climate*, *43*, 101161.
367 <https://doi.org/10.1016/j.uclim.2022.101161>
- 368 Goodman, S. J., Blakeslee, R. J., Koshak, W. J., Mach, D., Bailey, J., Buechler, D., Carey, L.,
369 Schultz, C., Bateman, M., McCaul, E., & Stano, G. (2013). The GOES-R Geostationary
370 Lightning Mapper (GLM). *Atmospheric Research*, *125–126*, 34–49.
371 <https://doi.org/10.1016/j.atmosres.2013.01.006>
- 372 Goodman, S., Mach, D., Koshak, W., & Blakeslee, R. (2012). *GLM Lightning Cluster-Filter*
373 *Algorithm*. 73.
- 374 Hayward, L., Whitworth, M., Pepin, N., & Dorling, S. (2020). Review article: A comprehensive
375 review of datasets and methodologies employed to produce thunderstorm climatologies.
376 *Natural Hazards and Earth System Sciences*, *20*(9), 2463–2482.
377 <https://doi.org/10.5194/nhess-20-2463-2020>
- 378 Huff, F. A., & Changnon, S. A. (1973). Precipitation modification by major urban areas. *Bulletin*
379 *of the American Meteorological Society*, *54*(12), 1220–1233. [https://doi.org/10.1175/1520-](https://doi.org/10.1175/1520-0477(1973)054<1220:PMBMUA>2.0.CO;2)
380 [0477\(1973\)054<1220:PMBMUA>2.0.CO;2](https://doi.org/10.1175/1520-0477(1973)054<1220:PMBMUA>2.0.CO;2)
- 381 Koshak, W., Mach, D., Bateman, M., Armstrong, P., & Virts, K. (2018). *Product Performance*
382 *Guide For Data Users*. 16.
- 383 Lay, E., Rodger, C., Holzworth, R., & Dowden, R. (2005). *Introduction to the World Wide*
384 *Lightning Location Network (WWLLN)*.
- 385 MacGorman, D. R., Apostolakopoulos, I. R., Lund, N. R., Demetriades, N. W. S., Murphy, M. J.,
386 & Krehbiel, P. R. (2011). The Timing of Cloud-to-Ground Lightning Relative to Total
387 Lightning Activity. *Monthly Weather Review*, *139*(12), 3871–3886.
388 <https://doi.org/10.1175/MWR-D-11-00047.1>
- 389 McLeod, J., & Shepherd, J. M. (2022). A Synoptic Framework for Forecasting the Urban Rainfall
390 Effect Using Composite and K-Means Cluster Analyses. *Frontiers in Environmental Science*,
391 *10*. <https://www.frontiersin.org/article/10.3389/fenvs.2022.808026>

- 392 McLeod, J., Shepherd, M., & Konrad, C. E. (2017). Spatio-temporal rainfall patterns around
393 Atlanta, Georgia and possible relationships to urban land cover. *Urban Climate*, *21*, 27–42.
394 <https://doi.org/10.1016/j.uclim.2017.03.004>
- 395 Medici, G., Cummins, K. L., Cecil, D. J., Koshak, W. J., & Rudlosky, S. D. (2017). The Intracloud
396 Lightning Fraction in the Contiguous United States. *Monthly Weather Review*, *145*(11),
397 4481–4499. <https://doi.org/10.1175/MWR-D-16-0426.1>
- 398 Miller, P., Ellis, A. W., & Keighton, S. (2015). Spatial distribution of lightning associated with
399 low-shear thunderstorm environments in the central Appalachian region. *Physical*
400 *Geography*, *36*(2), 127–141. <https://doi.org/10.1080/02723646.2015.1011257>
- 401 Oda, P. S. S., Enoré, D. P., Mattos, E. V., Gonçalves, W. A., & Albrecht, R. I. (2022). An initial
402 assessment of the distribution of total Flash Rate Density (FRD) in Brazil from GOES-16
403 Geostationary Lightning Mapper (GLM) observations. *Atmospheric Research*, *270*, 106081.
404 <https://doi.org/10.1016/j.atmosres.2022.106081>
- 405 Oke, T. R. (1982). The energetic basis of the urban heat island. *Quarterly Journal of the Royal*
406 *Meteorological Society*, *108*(455), 1–24. <https://doi.org/10.1002/qj.49710845502>
- 407 Orville, R. E., Huffines, G., Nielsen-Gammon, J., Zhang, R., Ely, B., Steiger, S., Phillips, S., Allen,
408 S., & Read, W. (2001). Enhancement of cloud-to-ground lightning over Houston, Texas.
409 *Geophysical Research Letters*, *28*(13), 2597–2600. <https://doi.org/10.1029/2001GL012990>
- 410 Pinto, I. R. C. A., Pinto, O. J., Gomes, M. a. S. S., & Ferreira, N. J. (2004). Urban effect on the
411 characteristics of cloud-to-ground lightning over Belo Horizonte-Brazil. *Annales*
412 *Geophysicae*, *22*(2), 697–700. <https://doi.org/10.5194/angeo-22-697-2004>
- 413 R Core Team. (2022). *R: A Language and Environment for Statistical Computing*. R Foundation
414 for Statistical Computing. <https://www.R-project.org/>
- 415 Rose, L., Stallins, J., & Bentley, M. (2008). Concurrent Cloud-to-Ground Lightning and
416 Precipitation Enhancement in the Atlanta, Georgia (United States), Urban Region. *Earth*
417 *Interactions - EARTH INTERACT*, *12*, 1–30. <https://doi.org/10.1175/2008EI265.1>
- 418 Rudlosky, S. (2020). *Geostationary Lightning Mapper Value Assessment*.
419 <https://doi.org/10.25923/2616-3V73>
- 420 Rudlosky, S. D., Goodman, S. J., Virts, K. S., & Bruning, E. C. (2019). Initial Geostationary
421 Lightning Mapper Observations. *Geophysical Research Letters*, *46*(2), 1097–1104.
422 <https://doi.org/10.1029/2018GL081052>

- 423 Schultz, M. D., Underwood, S. J., & Radhakrishnan, P. (2005). A Method to Identify the Optimal
424 Areal Unit for NLDN Cloud-to-Ground Lightning Flash Data Analysis. *Journal of Applied
425 Meteorology and Climatology*, 44(5), 739–744. <https://doi.org/10.1175/JAM2234.1>
- 426 Schulzweida, U. (2022). *CDO User Guide (2.1.0)*. Zenodo.
427 <https://doi.org/10.5281/zenodo.7112925>
- 428 Shepherd, M., Andersen, T., Strother, C., Horst, A., Bounoua, L., & Mitra, C. (2014). Urban
429 Climate Archipelagos: A new Framework for urban impacts on climate. *Earthzine*.
- 430 Shepherd, M., Stallins, J., Jin, M. L., & Mote, T. (2015). *Urbanization: Impacts on Clouds,
431 Precipitation, and Lightning* (pp. 1–28). <https://doi.org/10.2134/agronmonogr55.c1>
- 432 Snyder, J. P. (1987). *Map projections: A working manual*. USGS. <https://doi.org/10.3133/pp1395>
- 433 Stallins, J., & Bentley, M. (2006). Urban lightning climatology and GIS: An analytical framework
434 from the case study of Atlanta, Georgia. *Applied Geography*, 26, 242–259.
435 <https://doi.org/10.1016/j.apgeog.2006.09.008>
- 436 Stallins, J., Bentley, M., & Rose, L. (2006). Cloud-to-ground flash patterns for Atlanta, Georgia
437 (USA) from 1992 to 2003. *Climate Research - CLIMATE RES*, 30, 99–112.
438 <https://doi.org/10.3354/cr030099>
- 439 Stallins, J., Carpenter, J., Bentley, M., Ashley, W., & Mulholland, J. (2012). Weekend–weekday
440 aerosols and geographic variability in cloud-to-ground lightning for the urban region of
441 Atlanta, Georgia, USA. *Regional Environmental Change*, 13.
442 <https://doi.org/10.1007/s10113-012-0327-0>
- 443 Stallins, J., & Rose, L. (2008). Urban Lightning: Current Research, Methods, and the Geographical
444 Perspective. *Geography Compass*, 2, 620–639. [https://doi.org/10.1111/j.1749-
445 8198.2008.00110.x](https://doi.org/10.1111/j.1749-8198.2008.00110.x)
- 446 Student. (1908). The Probable Error of a Mean. *Biometrika*, 6(1), 1–25.
447 <https://doi.org/10.2307/2331554>
- 448 Thiel, K. C., Calhoun, K. M., Reinhart, A. E., & MacGorman, D. R. (2020). GLM and ABI
449 Characteristics of Severe and Convective Storms. *Journal of Geophysical Research:
450 Atmospheres*, 125(17), e2020JD032858. <https://doi.org/10.1029/2020JD032858>
- 451 Yang, L., Jin, S., Danielson, P., Homer, C., Gass, L., Bender, S. M., Case, A., Costello, C., Dewitz,
452 J., Fry, J., Funk, M., Granneman, B., Liknes, G. C., Rigge, M., & Xian, G. (2018). A new
453 generation of the United States National Land Cover Database: Requirements, research

454 priorities, design, and implementation strategies. *ISPRS Journal of Photogrammetry and*
455 *Remote Sensing*, 146, 108–123. <https://doi.org/10.1016/j.isprsjprs.2018.09.006>